

ICRH induced rotation in the tokamak TEXTOR

*S. Soldatov^{1 2}, A. Krämer-Flecken², E. Delabie⁴, M. Kantor^{2 3 4}, G. Van Wassenhove⁵
G. Van Oost¹*

¹Department of Applied Physics, Ghent University, 9000 Gent, Belgium

²Institute for Energy Research – Plasma Physics , Forschungszentrum Jülich GmbH, Association EURATOM-FZJ, D-52425 Jülich, Germany

³Ioffe Institute, RAS, Saint Petersburg 194021, Russia

⁴FOM-Institute for Plasma Physics Rijnhuizen , Association EURATOM-FOM, P.O. Box 1207, 3430 BE Nieuwegein, The Netherlands

⁵Laboratory for Plasma Physics , ERM/KMS, Association EURATOM-Belgian State, Brussels, Belgium
Partners in the Trilateral Euregio Cluster

Motivation. The external momentum input in ITER plasmas is expected to be limited and is not to be able to drive the plasma rotation much. In slow rotating plasmas the development of both a drift wave turbulence and resistive wall modes will deteriorate the confinement. It was reported from many experiments that externally launched electromagnetic rf waves are often accompanied by the generation of an additional torque in the plasma. This effect could be beneficial for a fusion reactor however, it still requires further understanding of the underlying physics to predict the intrinsic rotation for the next generation of fusion devices.

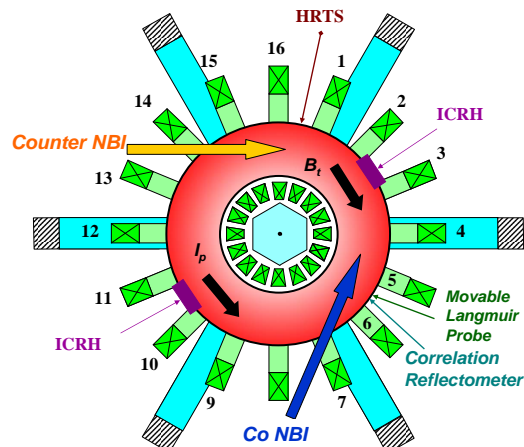


Figure 1: *TEXTOR top view with diagnostics and plasma heating systems displacement.*

Experimental results. TEXTOR is a middle size ($R=1.75$ m, $a=0.47$ m) tokamak with circular cross section and poloidal limiter. It is equipped with two tangential oppositely directed neutral beam injectors (NBI) each with 1.5 MW of maximum power and ion cyclotron resonance heating (ICRH) system with two antennas (each of 2 MW maximal power) is available for plasma auxiliary heating. The parameters of L-mode plasmas under investigation are as follows: plasma current/toroidal field I_p B_t 0.2 MA/1.9 T and 0.4 MA/2.5 T, averaged electron density n_e 1.8 2.2 $10^{19} m^{-3}$. Target deuterium plasmas were heated with two oppositely directed deuterium atomic beams and on-axis ICRH operating in the fundamental hydrogen minority heating scheme in

deuterium majority plasmas ($0.1 n_H n_D = 0.14$). The effect on the plasma rotation from ICRH was studied for plasmas with different toroidal rotation that was realized by adjusting the power of co- I_p NBI (P_{NBI}^{co}) and counter- I_p NBI ($P_{NBI}^{counter}$) (see Fig. 2). The toroidal plasma rotation, Ω_φ , was measured with CXRS system whereas the turbulence rotation perpendicular to magnetic field lines, v , associated with the rotation of plasma, was detected with Correlation Reflectometer (CR) [1]. The detailed plasma pressure profiles with a space resolution of 5 mm were provided by Thomson Scattering diagnostic [2]. Using the the radial balance force equation

$$E_r = \frac{\nabla p_i}{Z_i e n_i} = v \cdot B_{tot} = E_r^{dia} - E_r^{Lorentz} \quad (1)$$

and assuming $\nabla p_e = \nabla p_i$, the perpendicular rotation can be interpreted in the terms of radial electric field. Here, B_{tot} T_i p_i n_i Z_i are the total magnetic field strength, ion temperature, ion

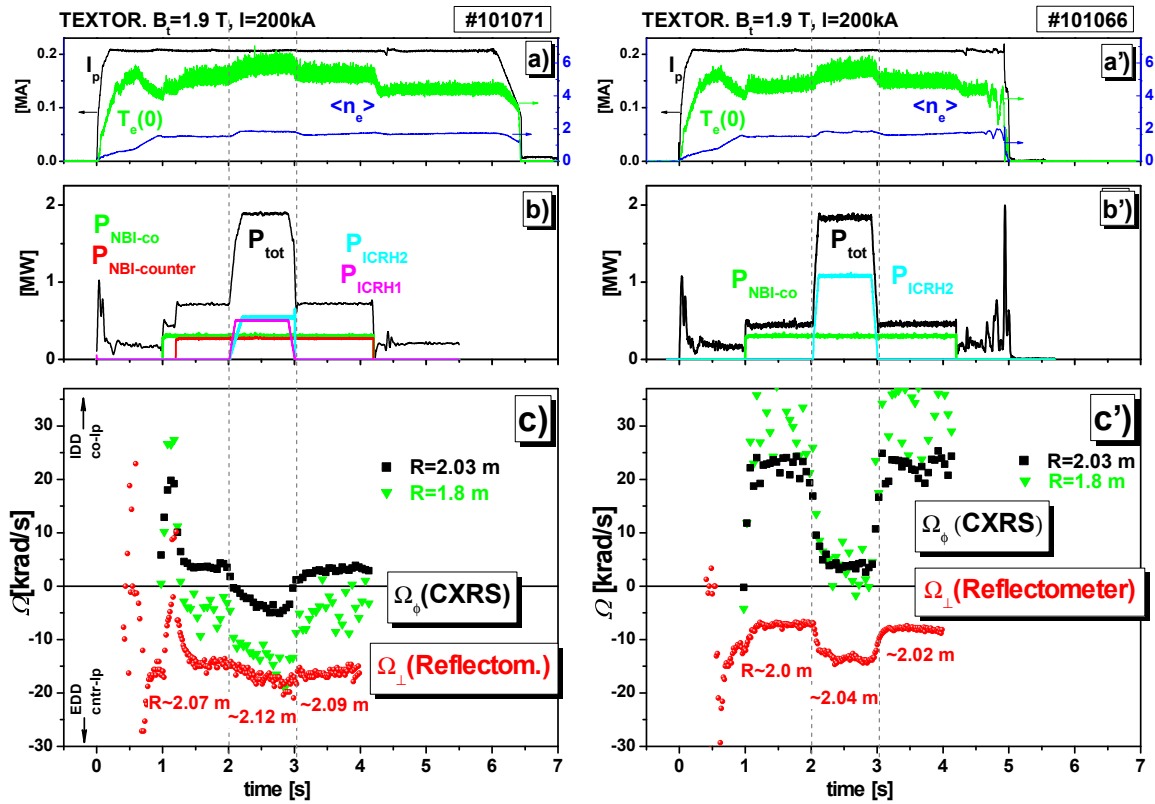


Figure 2: Time traces of the main plasma parameters, power of auxiliary heating and angular rotation are shown on the top, middle and lower graphs for two plasma scenarios.

pressure, ion density and ion charge respectively. E_r^{dia} and $E_r^{Lorentz}$ are the components of the electric field driven by ion diamagnetic flow and plasma net flow perpendicular to B_{tot} .

In TEXTOR the toroidal rotation of Ohmic heated plasmas is directed in the counter-I_p direction. Thus, the co-NBI brakes "Ohmic" plasma rotation (see Fig. 2 right lower graph) and counter-NBI accelerates it. Figure 2 shows that the application of ICRH is accompanied by the change both in Ω_ϕ and in Ω implying the changes in the plasma torque and/or in E_r . The effect on the rotation is smaller for balanced NBIs (left graph) as compared with preferable co-NBI heated plasmas (right graph). Note that the negative and positive values in Ω and Ω_ϕ correspond to electron/ion diamagnetic drift directions and counter- I_p /co- I_p directions respectively.

A detailed study on the ICRH induced rotation depending on the target plasma rotation was undertaken for plasmas with $I_p=0.4$ MW, $B_t=2.5$ T and $P_{NBI}^{co} = P_{NBI}^{counter} = 1$ MW (see Fig. 3 left graph). The power ratio co-NBI/counter-NBI was varied as follows 900/0; 600/300; 450/450 and 0/900 kW, thereby keeping net injected power constant. For every target plasma with particular P_{NBI}^{co} $P_{NBI}^{counter}$ ratio we have varied P_{ICRH} within 0–1000 kW. The results are summarized in Figures 3– 5. The time traces of Ω_ϕ are presented in Fig. 3, CXRS data corresponding to P_{ICRH} within 0–1000 kW are color coded as black-blue-green-magenta-red. One sees the effect from application of ICRH is counter- I_p directed and is maximal for plasmas heated preferably with co-NBI and deteriorates towards ones heated predominately with counter-NBI. Some deviations in Ω_ϕ traces in the discharges with P_{NBI}^{co} $P_{NBI}^{counter} = 600$ 300 kW are due to the breakdowns of the ICRH power happened during the operation. Figure 3(right graph) shows the deviation of the toroidal rotation $\Delta\Omega_\phi$ as an increasing function of P_{ICRH} for the case of P_{NBI}^{co} $P_{NBI}^{counter} = 600$ 300 kW by red squares.

The perpendicular angular rotation profiles Ω_\perp by CR for the same plasmas are presented in Fig. 4 for $P_{ICRH} = 300$ kW (left graph) and 800 kW (right graph) together with the refer-

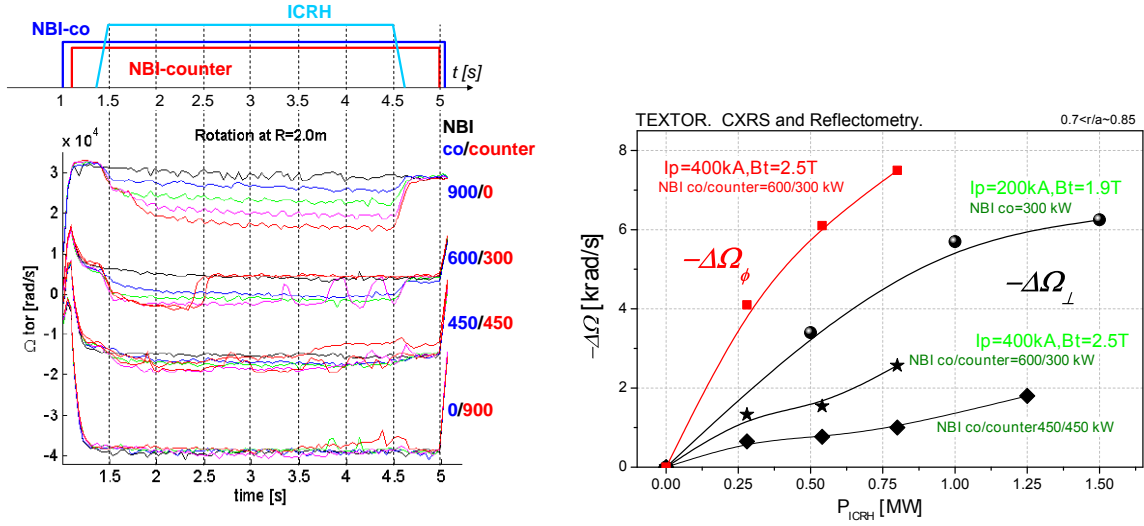


Figure 3: (left) Time traces of toroidal rotation measured during NBI and ICRH operation for four different relative co-NBI/counter-NBI ratios. (right) Changes in angular toroidal and perpendicular rotations measured with CXRS and CR versus P_{ICRH} for different plasmas.

ence profiles with $P_{\text{ICRH}} = 0$ displayed in thin lines and open symbols. Note that, for innermost plasma region ($\rho \approx 0.4$ m) $\Omega \approx \rho$ profiles change significantly with $P_{\text{NBI}}^{\text{co}}/P_{\text{NBI}}^{\text{counter}}$ following the projection Ω_ϕ to B direction [1, 3]. At the same time, the peripheral Ω is nearly independent both on the NBI and ICRH heating scenarios equating to ≈ 15 krad/s. This fact is understandable, while on the one hand the injected torque profile is maximal in the center, reduces towards the periphery and vanishes near the LCFS, and on the other hand the ∇p shows only small variations for plasmas under consideration (see $E_r^{\text{dia}} \approx \nabla p / n$ in Fig. 5). The changes in Ω as a function of P_{ICRH} averaged within $0.32 \leq \rho \leq 0.39$ m for $P_{\text{NBI}}^{\text{co}}/P_{\text{NBI}}^{\text{counter}} = 450/450$ and $600/300$ kW are depicted in Fig. 3(right graph). One sees the effect is stronger for higher

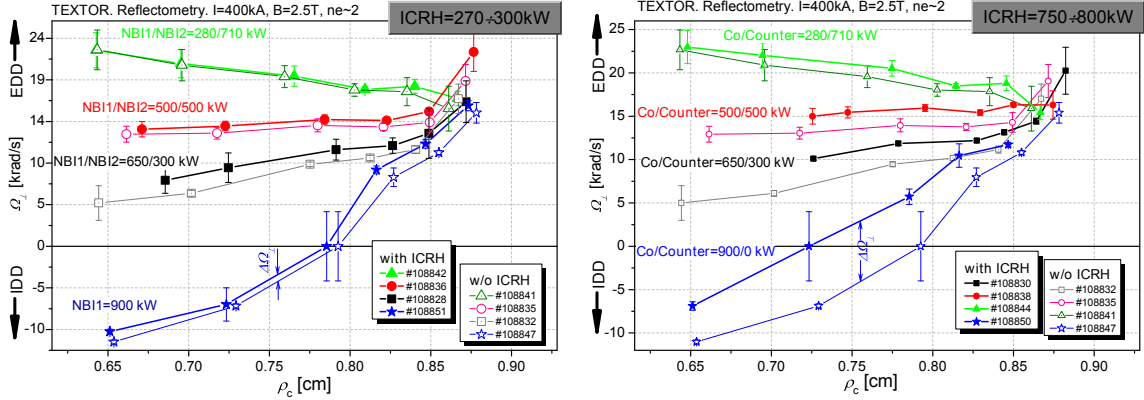


Figure 4: Turbulence perpendicular rotation profiles measured for different fractions of $P_{\text{co-NBI}}$ and $P_{\text{cntr-NBI}}$ ($P_{\text{co-NBI}} = P_{\text{cntr-NBI}} = \text{const}$). The reference profiles for plasmas without ICRH and with ICRH are depicted by thin lines with open symbols and thick lines with filled symbols respectively. (left) $P_{\text{ICRH}} = 270$ kW. (right) $P_{\text{ICRH}} = 780$ kW.

$P_{\text{NBI}}^{\text{co}}/P_{\text{NBI}}^{\text{counter}}$ but still lower as compared with $I_p/B_t=400\text{kA}/1.9\text{T}$ plasmas. Following the eq. 1 changes in Ω are associated with changes in radial electric field. In the framework of the assumption of $\nabla p_e \approx \nabla p_i$ we estimate both Lorentz and diamagnetic terms of E_r (see Fig. 5 left graph) as well as their sum $E_r^{\text{tot}} = E_r^{\text{Lorentz}} + E_r^{\text{dia}}$ (Fig. 5 right graph). The electron pressure profiles do not vary much, therefore the calculated E_r^{dia} ρ profiles (depicted in gray-scale) are very close for plasmas under consideration. At the same time E_r^{Lorentz} profiles vary both with $P_{\text{NBI}}^{\text{co}}/P_{\text{NBI}}^{\text{counter}}$ and with P_{ICRH} . The effect from ICRH application is well distinguished for

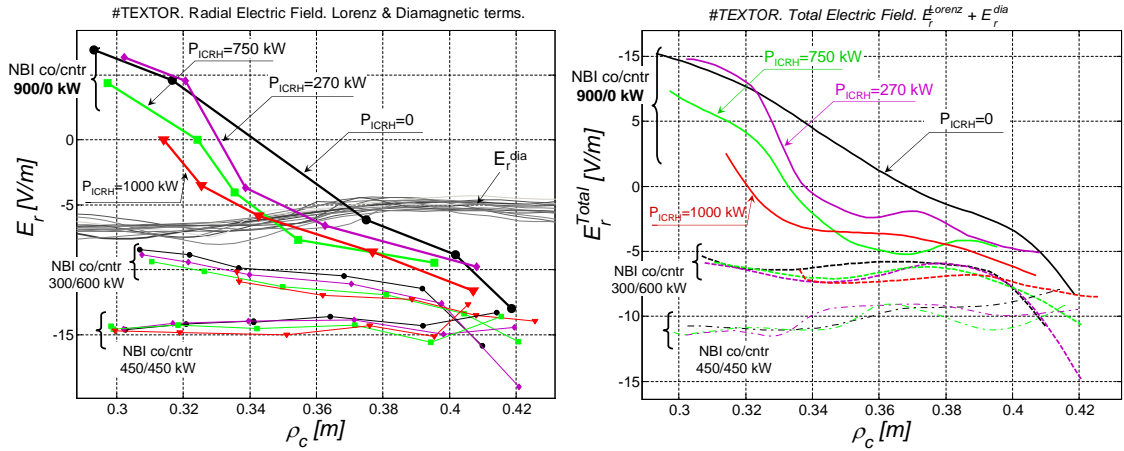


Figure 5: (left) Radial profiles of the Lorentz (colored curves with symbols) and diamagnetic (gray scale curves) terms of the radial electric field measured with CR and HRTS in different plasma heating scenarios. (right) The radial profile of the total electric field, $E_r^{\text{tot}} = E_r^{\text{Lorenz}} + E_r^{\text{dia}}$.

maximal P_{NBI}^{co} P_{NBI}^{counter} corresponding to predominate co-NBI (900 kW) heated target plasmas. The launching of the rf waves with $P=270\text{ kW}$ only reduces E_r^{tot} by $\Delta E_r^{\text{tot}} = 5 \text{ kV/m}$ but locally within $0.32 \leq \rho \leq 0.37 \text{ m}$. The radial range where E_r^{tot} is affected by ICRH application expands and E_r^{tot} deeps with the P_{ICRH} reaching at $P_{ICRH} = 980 \text{ kW}$ $8 \Delta E_r^{\text{tot}} = 3 \text{ kV/m}$ within $0.31 \leq \rho \leq 0.41 \text{ m}$ radial range.

Discussion. The application of ICRH leads to an acceleration of plasma rotation both in electron diamagnetic drift direction and in toroidal counter-Ip direction. It is found that the effect of ICRH induced rotation increases with P_{ICRH} however, it reveals nonlinear saturation (Fig. 3). Furthermore, the higher P_{NBI}^{co} P_{NBI}^{counter} P_{NBI}^{co} ratio, the larger effect of the ICRH induced rotation. The estimated radial electric field profiles indicate the decrease of electric field in the region $0.3 \leq \rho \leq 0.4 \text{ m}$ ($0.65 \leq \rho \leq 0.85$) by $8 \Delta E_r = 3 \text{ kV/m}$. Such a deepening of the E_r profiles could originate form an electric charge redistribution in the plasma volume. The possible effect of energetic ion losses, that could explain the decrease in E_r , is expected mostly from the central region ($\rho = 0.2 \text{ m}$) according to the power deposition profiles [4]. It seems to contradict our findings of nearly local deepening of E_r within $0.32 \leq \rho \leq 0.37$ for a small level of ICRH that extends to $0.3 \leq \rho \leq 0.4 \text{ m}$ for higher P_{ICRH} . The observed dependency of ICRH induced rotation on the P_{NBI}^{co} P_{NBI}^{counter} P_{NBI}^{co} ratio could result from the different effects accompanying the heating with co and counter NBI. One of them is i) the different profiles of the trapped hot ions and ii) the current drive [5]. Moreover, the changes in the distribution function and even slowing down of the beam due to ICRH application considered in [4] may play a role. In general, the effect is more pronounced for plasmas with $I_p/B_t = 200 \text{ kA}/1.9 \text{ T}$ as compared with $I_p/B_t = 400 \text{ kA}/2.5 \text{ T}$ that could be a consequence of the difference in the mode conversion mechanism which suppose to be sensitive to poloidal and toroidal fields in a tokamak.

References

- [1] A. Kraemer-Flecken et al. *Nucl. Fusion*, 44:1143–1157, 2004.
- [2] M. Kantor et al. *Plasma Phys. Control. Fusion*, 51:055002, 2009.
- [3] S. Soldatov et al. *Plasma Phys. Control. Fusion*, to be published, 2010.
- [4] A.M. Messiaen et al. *Plasma Phys. Control. Fusion*, 35:A15–A34, 1993.
- [5] A.M. Messiaen et al. *Plasma Phys. Control. Fusion*, 32:889–902, 1990.